JACS
JOURNAL OF THE AMERICAN CHEMICAL SOCIETY
Communication
pubs.acs.org/JACS

Photocatalytic Hydrogen Evolution from FeMoS-Based Biomimetic Chalcogels

Benjamin D. Yuhas,[†] Amanda L. Smeigh,[†] Alexios P. Douvalis,[‡] Michael R. Wasielewski,[†] and Mercouri G. Kanatzidis*,[†]

[†]Department of Chemistry and Argonne-Northwestern Solar Energy Research (ANSER) Center, Northwestern University, Evanston, Illinois 60208, United States

[‡]Department of Physics, University of Ioannina, 45110 Ioannina, Greece

Supporting Information

ABSTRACT: The naturally abundant elements used to catalyze photochemical processes in biology have inspired many research efforts into artificial analogues capable of proton reduction or water oxidation under solar illumination. Most biomimetic systems are isolated molecular units, lacking the protective encapsulation afforded by a protein's tertiary structure. As such, advances in biomimetic catalysis must also be driven by the controlled integration of molecular catalysts into larger superstructures. Here, we present porous chalcogenide framework materials that contain biomimetic catalyst groups immobilized in a chalcogenide network. The chalcogels are formed via metathesis reaction between the clusters $[Mo_2Fe_6S_8(SPh)_3Cl_6]^{3-}$ and $[Sn_2S_6]^{4-}$ in solution, yielding an extended, porous framework structure with strong optical absorption, high surface area (up to 150 m^2/g), and excellent aqueous stability. Using $[Ru(bpy)_3]^{2+}$ as the light-harvesting antenna, the chalcogels are capable of photocatalytically producing hydrogen from mixed aqueous solutions and are stable under constant illumination over a period of at least 3 weeks. We also present improved hydrogen yields in the context of the energy landscape of the chalcogels.

One of the principal challenges in the large-scale implementation of solar fuel technology is the design and fabrication of suitable catalysts from abundant and inexpensive constituent elements.[1−4] For this reason, many researchers have used nature as inspiration for catalyst design, mimicking the naturally abundant elements found in proteins.[5,6] Biomimetic catalysis is currently an active research area; however, most biomimetic species are isolated, molecular systems.[7−10] These molecules may or may not be faithful analogues of enzyme active centers, and some show interesting catalytic activity, but they also lack the protective equivalent of the protein backbone. Consequently, many of these catalysts suffer from greatly shortened lifetimes, although there have been recent advances in this area.[11] However, an additional goal of biomimetic catalysis must be not only the identification of potential catalysts but also their *controlled integration* into larger structures.

We have recently introduced a new class of porous chalcogenide materials, dubbed chalcogels.[12,13] Unlike the majority of porous inorganic materials, which are based on oxides, chalcogels are made from sulfides, selenides, or tellurides, which allows for the synthesis of materials with tunable, visible light absorption as well as highly polarizable surfaces and excellent surface areas. Furthermore, chalcogels can be functionalized with subunits similar to those found in biomolecules, such as redox-active cluster units and light-harvesting moieties, all fully integrated into a semiconducting chalcogenide scaffold.[14,15] Here, we present biomimetic chalcogels capable of photocatalytic hydrogen evolution under simulated solar illumination. Demonstrating the chemical versatility inherent in our novel chalcogel synthetic method, the new chalcogels are prepared from double-cubane $Mo_2Fe_6S_8$ cluster units linked by Sn_2S_6 ligands, forming a random, amorphous network with strong optical absorption. The switch from Fe_4S_4 cubane units to $Mo_2Fe_6S_8$ double-cubane units illustrates the flexibility and ease with which we can synthesize chalcogels with a variety of redox-active biomimetic cofactors. The chalcogels can be easily functionalized with cationic chromophores, such as $[Ru(bpy)_3]^{2+}$, enabling photoexcited electron transfer from dye to cluster. The biomimetic chalcogels are fully stable in aqueous solutions under illumination for at least 3 weeks, which contrasts greatly with the water-unstable molecular $[Mo_2Fe_6S_8]$-based clusters. Our new generation of MoFeS-based chalcogels is superior in performance to our first-generation Fe_4S_4-based chalcogels,[14,15] and we rationalize this improvement based on spectroscopic and electrochemical characterization.

Molecular iron−molybdenum cofactor analogues have been known for some time,[7,8] and some reports exist on their H_2-producing capabilities,[16,17] although none in a photochemical setting. Additionally, the nitrogenase protein, with its FeMo cofactor, has also been shown to be a catalyst for hydrogen production, which can occur concurrently with nitrogen reduction to ammonia.[18−22] With suitable terminal ligands, the $Mo_2Fe_6S_8$ clusters can be cross-linked with Sn_2S_6 clusters to form a polymeric and porous chalcogenide framework, as envisioned in Scheme 1. The reaction proceeds from the metathesis displacement of the terminal Cl^- ligands in the cluster[23] $[Mo_2Fe_6S_8Cl_6(SPh)_3]^{3-}$ by the terminal sulfides of

Received: April 16, 2012
Published: June 4, 2012

   dx.doi.org/10.1021/ja303640s | J. Am. Chem. Soc. 2012, 134, 10353−10356

Scheme 1. Synthesis of $Mo_2Fe_6S_8$–Sn_2S_6 Chalcogels

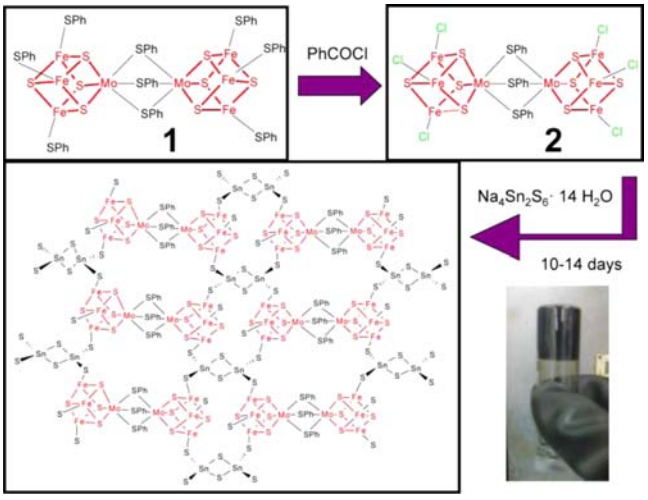

$[Sn_2S_6]^{4-}$. After 10–14 days of standing at room temperature, this reaction results in a black chalcogel.

Electron microscopy (Figure 1A, B) reveals the spongy, porous nature of the chalcogels, which always appear

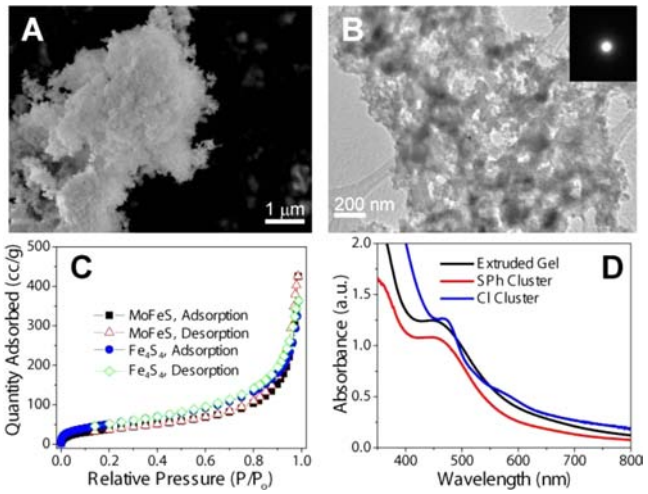

Figure 1. (A,B) Scanning and transmission electron micrographs of a representative MoFeS chalcogel. The inset in panel B shows a typical chalcogel SAED pattern, revealing its amorphous nature. (C) Nitrogen adsorption/desorption isotherms obtained at 77 K of MoFeS- and Fe_4S_4-based chalcogels. (D) UV–vis spectra in DMF of clusters **1** and **2** (see Scheme 1) as well as a MoFeS chalcogel that has been exposed to excess benzenethiol.

amorphous as determined from TEM and XRD experiments. Energy dispersive spectroscopy (EDS) was used to determine the elemental composition of the chalcogels, which leads to an approximate chalcogel empirical formula of $[Mo_2Fe_6S_8]$-$[Sn_2S_6]_{1.25}$. (Details in Supporting Information (SI), Figure S1). Nitrogen adsorption/desorption measurements (Figure 1C) on the chalcogels exhibit similar isotherm characteristics[24] to previously described chalcogels containing the Fe_4S_4 cubane cluster[14] instead of the $Mo_2Fe_6S_8$ double cubane clusters, with pore sizes ranging from 6.3 to 75 Å. Although the absolute surface areas of the $Mo_2Fe_6S_8$-based chalcogels are lower than that of Fe_4S_4-based chalcogels (average values are 144 and 192 m^2/g, respectively), this can be explained by the presence of the heavier molybdenum atoms.

The clusters in the chalcogels were characterized by a variety of means. Thiol extrusion experiments were used to confirm the intact structure of the $Mo_2Fe_6S_8$ clusters. Normally, the chalcogels are stable in many solvents, including water, without dissolution or leaching. However, if a large excess of benzenethiol is added to the solution, the gels dissolve rapidly, as the $Mo_2Fe_6S_8$ cluster is extruded from the gel by the benzenethiol, yielding the $[Mo_2Fe_6S_8(SPh)_9]^{3-}$ anion in solution. UV–vis spectra for the molecular clusters and the extruded chalcogel solution are shown in Figure 1D; the characteristic absorption maxima agree well with the established literature.[7,8]

The electronic properties of the MoFeS chalcogels were examined by solid-state cyclic voltammetry (CV) experiments. Figure 2A shows a typical CV curve obtained from the wet

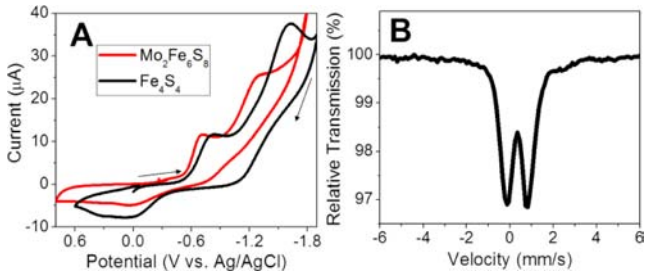

Figure 2. (A) Representative solid-state CV of MoFeS chalcogels and Fe_4S_4 chalcogels, recorded in MeCN at 60 mV/s with $(NBu_4)PF_6$ as the supporting electrolyte. (B) ^{57}Fe Mossbauer of MoFeS chalcogel measured at 10 K.

chalcogel immobilized on the surface of the working electrode by a doctor-blade technique. Two distinct reduction waves are observed in the chalcogels, occurring at approximately −700 and −1400 mV, indicating that the MoFeS clusters in the chalcogel network are redox active. These reduction potentials are in agreement with previous experiments performed in solution on MoFeS molecular clusters.[7,8] Furthermore, these reduction potentials are less negative than those observed in Fe_4S_4-based chalcogels.[14] ^{57}Fe Mössbauer spectroscopy (Figure 2B) of the chalcogels supports the presence of the MoFeS clusters in the structures. The spectra show a major central quadrupole splitting contribution at all measured temperatures. This contribution was fitted using two very similar quadrupole doublets, whose resulting isomer shifts of 0.44 and 0.43 mm/s (relative to metallic iron at room temperature) and quadrupole splittings of 1.24 and 0.78 mm/s at 10 K are consistent with those previously reported[8,25] for the reduced $[Mo_2Fe_6S_8(SPh)_9]^{n-}$ double cubane clusters (Table S1, Supporting Information), suggesting an intermediate oxidation state for iron close to or less than $Fe^{2.5+}$. The temperature evolution of the Mössbauer spectra from room temperature down to 10 K and the resulting hyperfine parameters indicate that the cluster environment is highly uniform throughout the chalcogel.

The photochemical hydrogen-evolving ability of the MoFeS-based chalcogels was tested in mixed solutions of acetonitrile:-water (4:1 v/v), using 2,6-lutidine hydrochloride and sodium ascorbate as the proton and electron source, respectively. The samples were sealed under nitrogen and continually illuminated with a 150 W xenon lamp equipped with an AM 1.5 filter. The

dx.doi.org/10.1021/ja303640s | J. Am. Chem. Soc. 2012, 134, 10353–10356

light intensity at the sample was 100 mW/cm^2. At certain intervals, the headspace in the vial was sampled for H_2 by gas chromatography. Figure 3A shows the H_2 production from

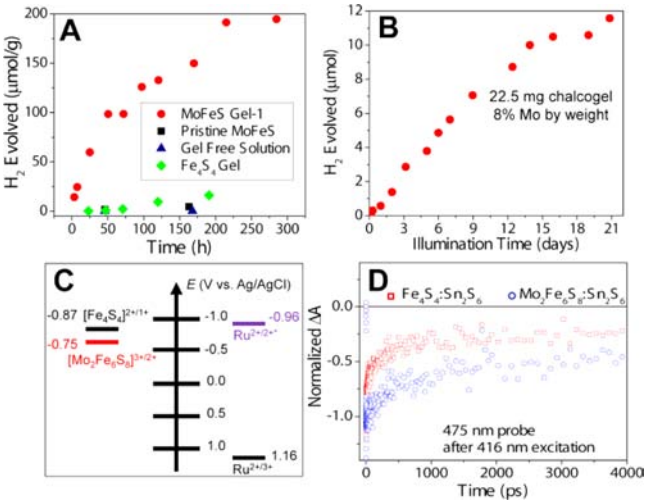

Figure 3. (A) Photochemical hydrogen evolution of $[Ru(bpy)_3]^{2+}$-functionalized MoFeS chalcogels, compared with functionalized Fe_4S_4 gels, pristine MoFeS gels (i.e., gels without $[Ru(bpy)_3]^{2+}$ present), and an illuminated gel-free solution. The hydrogen output is normalized to the mass of chalcogel present in the experiment. (B) Long-term hydrogen evolution of dye-functionalized MoFeS chalcogels, leading to a calculated turnover number of 1.2. (C) Energy diagram for electron transfer between excited $[Ru(bpy)_3]^{2+}$ and the clusters in the MoFeS and Fe_4S_4-based chalcogels. (D) Femtosecond transient absorption probing the ground-state bleach of $Ru(bpy)_3^{2+}$ in both MoFeS and Fe_4S_4-based chalcogels.

$[Ru(bpy)_3]^{2+}$-functionalized MoFeS-based chalcogels compared to the first-generation Fe_4S_4-based chalcogels as well as pristine (i.e., without dye functionalization) MoFeS chalcogels. The performance of the $[Ru(bpy)_3]^{2+}$-functionalized MoFeS chalcogels is far superior to that of their Fe_4S_4-based counterparts, and the pristine MoFeS chalcogels showed minimal hydrogen output.

The hydrogen evolution rate is remarkably consistent over long periods of time (Figure 3B), which illustrates the overall stability of the clusters in the chalcogels. The chalcogels were illuminated continuously for 21 days with no degradation in performance, resulting in a maximum hydrogen yield of 11.3 μmol H_2. This compares to 9.4 μmol of $Mo_2Fe_6S_8$ clusters in the chalcogel (determined from the chalcogel mass and elemental analysis), yielding a calculated turnover number of 1.2. However, this turnover number is a very underestimated lower bound, because this calculation assumes that all of the MoFeS clusters in the chalcogel are participating in the photochemical reaction. In reality, this is far from the case. Because of the strong optical absorption, and therefore limited light penetration, at the gel surface, only the exterior surface of the chalcogel is illuminated. Based on optical extinction measurements (SI, Figure S2), we estimate that less than 5% of the clusters are in fact illuminated by the incident light.

The improved hydrogen-evolving performance relative to the Fe_4S_4-based chalcogels can be explained by comparing the relative energies involved in the electron-transfer process. As shown in Figure 3C, the more anodic reduction potentials observed in the MoFeS-based chalcogels create a more favorable energy landscape and a greater driving force for electron transfer from the photoexcited $[Ru(bpy)_3]^{2+}$ to the $Mo_2Fe_6S_8$ cluster.[14,26] We further explored the electron-transfer process between chromophore and cluster with femtosecond transient absorption. Figure 3D shows the ground-state bleach of the $[Ru(bpy)_3]^{2+}$ dye when functionalized in the MoFeS chalcogels and the first-generation Fe_4S_4 chalcogels. The recovery of the $[Ru(bpy)_3]^{2+}$ ground state is seen to be much more rapid in the Fe_4S_4 chalcogels than in the MoFeS chalcogels. This suggests the possibility that the charge-separated state of the chromophore has a longer lifetime in the MoFeS chalcogels than in the Fe_4S_4 chalcogels, which is favorable for increased hydrogen output. Additionally, the increased shelf amplitude seen in the MoFeS chalcogels suggests that the $[Ru(bpy)_3]^{2+}$ excited state persists for a longer time as well. Further experiments are in progress to determine more accurately the electron-transfer pathways in this complex system. However, our current results suggest that both processes, i.e., a longer-lived chromophore excited state as well as a suppressed recombination rate of the chromophore, can allow for a longer-lived reduced MoFeS cluster and an ultimately more favorable scenario for the reduction of protons to H_2.

The superior and long-lived photocatalytic performance of our MoFeS chalcogels represents not only a significant advance in biomimetic catalysis but also the rational design of multifunctional complex porous systems. Our biomimetic chalcogels, containing redox-active subunits directly and covalently integrated into a protective scaffold, are stable in water under solar illumination, in stark contrast to similar molecular biomimetic catalysts, and can be thought of as solid-state protein analogues. We have shown through a variety of structural, electronic, and spectroscopic characterizations the delicate interplay between light-harvesting and catalytic subunits in a common superstructure. By constructing a chalcogel with more favorable reduction potentials for hydrogen production, as well as enhanced transient absorption characteristics, we see great improvements in overall catalyst performance. As the chalcogel chemistry described here is quite adaptable to a wide variety of cluster units, both biomimetic and main-group, we envision that these materials could be improved even further as well as tailored toward the photodriven transformations of more complex substrates.

■ ASSOCIATED CONTENT

Ⓢ Supporting Information

Detailed experimental parameters, chalcogel elemental analysis, Mössbauer parameters, and optical extinction data. This material is available free of charge via the Internet at http://pubs.acs.org.

■ AUTHOR INFORMATION

Corresponding Author

m-kanatzidis@northwestern.edu

Notes

The authors declare no competing financial interest.

■ ACKNOWLEDGMENTS

We thank Prof. Joseph Hupp for use of electrochemistry equipment. Electron microscopy and elemental analysis was performed at the Electron Probe Instrumentation Center at Northwestern University. This work was supported as part of the ANSER Center, an Energy Frontier Research Center

funded by the U.S. Department of Energy, Office of Science, Office of Basic Energy Sciences, under award no. DE-SC0001059.

REFERENCES

(1) Gray, H. B. *Nat. Chem.* **2009**, *1*, 7.
(2) Reece, S. Y.; Hamel, J. A.; Sung, K.; Jarvi, T. D.; Esswein, A. J.; Pijpers, J. J. H.; Nocera, D. G. *Science* **2011**, *334*, 645.
(3) Gust, D.; Moore, T. A.; Moore, A. L. *Acc. Chem. Res.* **2009**, *42*, 1890.
(4) Maeda, K.; Teramura, K.; Lu, D.; Takata, T.; Saito, N.; Inoue, Y.; Domen, K. *Nature* **2006**, *440*, 295.
(5) Kanan, M. W.; Nocera, D. G. *Science* **2008**, *321*, 1072.
(6) Najafpour, M. M.; Ehrenberg, T.; Wiechen, M.; Kurz, P. *Angew. Chem., Int. Ed.* **2010**, *49*, 2233.
(7) (a) Koutmos, M.; Georgakaki, I. P.; Coucouvanis, D. *Inorg. Chem.* **2006**, *45*, 3648. (b) Coucouvanis, D.; Kanatzidis, M.; Simhon, E.; Baenziger, N. C. *J. Am. Chem. Soc.* **1982**, *104*, 1874. (c) Kanatzidis, M. G.; Baenziger, N. C.; Coucouvanis, D.; Simopoulos, A.; Kostikas, A. *J. Am. Chem. Soc.* **1984**, *106*, 4500.
(8) Mascharak, P. K.; Papaefthymiou, G. C.; Armstrong, W. H.; Foner, S.; Frankel, R. B.; Holm, R. H. *Inorg. Chem.* **1983**, *22*, 2851.
(9) Tard, C.; Pickett, C. J. *Chem. Rev.* **2009**, *109*, 2245.
(10) (a) Gloaguen, F.; Lawrence, J. D.; Rauchfuss, T. B. *J. Am. Chem. Soc.* **2001**, *123*, 9476. (b) Kanatzidis, M. G.; Coucouvanis, D.; Simopoulos, A.; Kostikas, A.; Papaefthymiou, V. *J. Am. Chem. Soc.* **1985**, *107*, 4925.
(11) Helm, M. L.; Stewart, M. P.; Bullock, R. M.; DuBois, M. R.; Dubois, D. L. *Science* **2011**, *333*, 863.
(12) Bag, S.; Trikalitis, P. N.; Chupas, P. J.; Armatas, G. S.; Kanatzidis, M. G. *Science* **2007**, *317*, 490.
(13) Bag, S.; Gaudette, A. F.; Bussell, M. E.; Kanatzidis, M. G. *Nat. Chem.* **2009**, *1*, 217.
(14) Yuhas, B. D.; Smeigh, A. L.; Samuel, A. P. S.; Shim, Y.; Bag, S.; Douvalis, A. P.; Wasielewski, M. R.; Kanatzidis, M. G. *J. Am. Chem. Soc.* **2011**, *133*, 7252.
(15) Yuhas, B. D.; Prasittichai, C.; Hupp, J. T.; Kanatzidis, M. G. *J. Am. Chem. Soc.* **2011**, *133*, 15854.
(16) Christou, G.; Hageman, R. V.; Holm, R. H. *J. Am. Chem. Soc.* **1980**, *102*, 7600.
(17) Yamamura, T.; Christou, G.; Holm, R. H. *Inorg. Chem.* **1983**, *22*, 939.
(18) Seefeldt, L. C.; Hoffman, B. M.; Dean, D. R. *Annu. Rev. Biochem.* **2009**, *78*, 701.
(19) Roth, L. E.; Nguyen, J. C.; Tezcan, F. A. *J. Am. Chem. Soc.* **2010**, *132*, 13672.
(20) Dos Santos, P. C.; Igarashi, R. Y.; Lee, H.-I.; Hoffman, B. M.; Seefeldt, L. C.; Dean, D. R. *Acc. Chem. Res.* **2005**, *38*, 208.
(21) Burgess, B. K.; Lowe, D. J. *Chem. Rev.* **1996**, *96*, 2983.
(22) Einsle, O.; Tezcan, F. A.; Andrade, S. L. A.; Schmid, B.; Yoshida, M.; Howard, J. B.; Rees, D. C. *Science* **2002**, *297*, 1696.
(23) Christou, G.; Garner, C. D. *J. Chem. Soc., Chem. Commun.* **1980**, 613.
(24) Sing, K. S. W.; Everett, D. H.; Haul, R. A. W.; Moscou, L.; Pierotti, R. A.; Rouquerol, J.; Siemieniwska, T. *Pure Appl. Chem.* **1985**, *57*, 603.
(25) Christou, G.; Mascharak, P. K.; Armstrong, W. H.; Papaefthymiou, G. C.; Frankel, R. B.; Holm, R. H. *J. Am. Chem. Soc.* **1982**, *104*, 2820.
(26) Morandeira, A.; Fortage, J.; Edvinsson, T.; Le Pleux, L.; Blart, E.; Boschloo, G.; Hagfeldt, A.; Hammarström, L.; Odobel, F. *J. Phys. Chem. C* **2008**, *112*, 1721.